RSC Advances

ROYAL SOCIETY OF CHEMISTRY

www.rsc.org/advances

Development and characterization of a novel Swarna-based herbo-metallic colloidal nano-formulation – inhibitor of *Streptococcus mutans* quorum sensing

Brahma N. Singh[a]*[†], Prateeksha[a], Garima Pandey[a], Vishwjeet Jadaun[a], Sweta. Singh[a], Rajesh Bajpai[b], Sanjeeva Nayaka[b], Alim H. Naqvi[c], Ajay K.Singh Rawat[a]*, Dulip K. Upreti[b]* and Braj R. Singh[c]*[†]

[a]Pharmacognosy & Ethnopharmacology Division, CSIR-National Botanical Research Institute, Lucknow-226001, U.P., India. [b]Lichenology laboratory, Plant Biodiversity and Conservation Biology Division. CSIR-National Botanical Research Institute, Lucknow-226001, U.P., India. [c]Centre of Excellence in Materials Science (Nanomaterials), Department of Applied Physics, Z.H. College of Engineering & Technology, Aligarh Muslim University, Aligarh, U.P., India.

Keywords: Herbo-metallic colloidal nano-formulation; Swarna nanoparticles, Anti-quorum sensing activity, Virulence factors, Anti-biofilm activity

[†] These authors contributed equally.

*Corresponding authors:
B.N. Singh (singhbrahmanand99@gmail.com)
AKS Rawat (rawataks@rediffmail.com)
DK Upreti (upretidknbri@gmail.com)
B.R. Singh (brajviro@gmail.com)

Herbo-metallic preparations such as bhasmas (ash) are being traditionally used in Indian and Chinese medicinal systems. In Ayurveda, Swarna (gold) nanoparticles are used as Swarna Bhasma to treat several clinical manifestations. While, *Usnea longissima*, a medicinal lichen ethno-botanically is known for the treatment of tooth cleaning and infectious diseases. The study aims to develop a herbo-metallic colloidal nano-formulation containing Swarna nanoparticles and polyphenols rich *U. longissima* extract (ULE) and evaluation of its anti-quorum sensing (QS) property against *Streptococcus mutans* never explored before, with a view towards combating the emergence of antibiotic resistance often linked with QS-regulated virulence factors and biofilms. The synthesized Uh-Au@Nano-CF was confirmed by a peak at 550 nm in the UV–visible spectrum. The obtained XRD data confirmed the crystalline nature of nanoparticles of 28 nm size. TEM image revealed that all particles were spherical with a narrow size range of 5–23 nm. The FTIR result clearly showed that the ULE containing secondary OH as functional groups induces encapsulation of nanoparticles. HPTLC and HPLC fingerprinting of ULE confirmed the presence of polyphenols including orcinol, arabitol, apigenin, and usnic acid. The data from inhibition of violacein production in *C. violaceum* 12472 revealed that the Uh-Au@Nano-CF at sub-lethal concentrations (5, 10 and 15%) show potent anti-QS activity. The treatment of Uh-Au@Nano-CF was found to inhibit the secretion of *S. mutans* virulence factors, including acid production, ATPase, enolase, lactate dehydrogenase, protease, total exopolysaccharide content, and glucosidase. The Uh-Au@Nano-CF in a concentration dependent manner showed anti-biofilm activity, inhibiting biofilm formation. Eventually, it was also documented that the Uh-Au@Nano-CF at 15% dilution enhanced the susceptibility of *S. mutans* towards to its conventional antibiotics. This study introduces not only a novel antimicrobial herbo-metallic colloidal

nano-formulation, but also explores its new biomedical application targeting QS-regulated virulence factors and biofilm of *S. mutans* rather than its viability.

1 Introduction

Herbo-metallic formulations are being traditionally used in Indian and Chinese medicines and have several benefits including better stability, lower dosage, ease of storability and sustained availability [1]. These have been instrumental in their widespread use in treatment of different disorders by traditional medicinal practitioners. In Ayurveda (ancient Indian system of natural and holistic medicine), formulations containing metals called as bhasmas (ash containing metals and medicinal herbs) are very common [2]. Bhasma is unique ayurvedic metallic formulations prepared with herbal extracts or decoction, and ignited for certain quantum of heat as per puta (calcination) system of Ayurveda [3]. It is believed that the metal upon such special treatment processes gets converted to a bio-assimilable and nontoxic form. Naga bhasma (lead sulphide ash), Swarna bhasma (gold ash probably in nano form), and *Ba-pao-neu-hwang-san* (a Chinese traditional ash) are examples of traditional herbo-metallic preparations contained metals and several herbal ingredients, have been used as oral medicines for the treatment of diabetes, spleen enlargement, diarrhea, various kind of skin diseases, regulating blood strain, and relieve ache [1].

From ancient times, gold has been used either as Swarna bhasma in vedic era in India to manage several clinical manifestations including loss of memory, defective eyesight, infertility, overall body weakness and incidence of early aging [4]. Swarna bhasma has been used by Ayurvedic physicians to treat different diseases like tuberculosis, cancer, sterility, bronchial asthma, rheumatoid arthritis, aging, diabetes mellitus, anemia, cough, debility, nervous disorders, and muscular dystrophy etc. [5, 6]. Moreover, the ethno-botanical uses of *Usnea* species, a group of medicinal lichens is known for the treatment of tooth cleaning, infectious diseases, and gastric ulcer etc. [7-9]. Owing to vital role of Swarna bhasma and *Usnea* species in Ayurvedic medicine an effort to develop a herbo-metallic

preparation is aiming the present study which is an economic protocol to provide Swarna and lichen extract in a new colloidal nano form and opening avenue to explore its new biomedical application(s).

It is well documented that the emergence of antibiotic-resistant bacterial strains is increasing at an alarming pace. Unfortunately, these microbes continue to adapt more rapidly than new therapeutic agents can be developed to control them. However, medical community is now realizing on an appealing approach to this problem which targets bacterial cell-to-cell communication system associated with their virulence behaviors rather than essential cellular processes. Almost all bacteria use a hierarchical quorum sensing (QS) systems to regulate tolerance to multiple antibiotics and virulence behaviors [10-12]. Tooth decay is one of the most common disease in human, being at the top of the list of diseases related to QS-regulated biofilm formation [13]. *Streptococcus mutans* is the leading aetiological agent causing dental caries worldwide and is considered to be the most cariogenic of all of the oral streptococci [14, 15]. The production of QS-controlled virulence factors and biofilms development is recognized as important pathogenicity weapons in this bacterium [16-18]. The general therapeutic drugs towards dental decay are to use conventional antibiotics to treat underlying infection. But, *S. mutans* within biofilms are significantly less susceptible to antibiotics and antimicrobial stressors than are planktonic stage [19, 20]. The overarching goal of developing a new treatment for the leading dental carie-causing *S. mutans*, the discovery of QS inhibitors provides an avenue for inhibiting virulence of this bacterium.

Advances in nanotechnology have given rise to the rapid development of novel nanomaterials for their applications in biomedicine [21, 22]. Therefore, searching for potential nanomaterials with anti-QS and anti-biofilm activities may also be an attractive alternative to conventional antibiotics. Identification of such QS inhibitors could present us with new opportunities for the development of next-generation antimicrobials. In this sense, the anti-biofilm activity against a range of bacteria has

been described for Swarna nanoparticles and polyphenols from *U. longissima* [23-28], can be a potential source of QS-blockers or novel antimicrobial agents. However, to the best of our knowledge, no study exploring the anti-QS potential of Swarna-based herbo-metallic nano-formulation against *S. mutans* has been published.

Taking this into account, it seemed reasonable to develop a novel herbo-metallic colloidal nano-formulation (denoted as "Uh-Au@Nano-CF") containing Swarna nanoparticles and polyphenols rich extract of *U. longissima*, could have anti-QS and anti-biofilm properties. With this hypothesis, the aim of this study is to evaluate whether our developed Uh-Au@Nano-CF could inhibit the secretion of QS-regulated virulence factors and prevent biofilm formation in *S. mutans*.

2 Materials and methods

2.1 Materials

Chloroauric acid ($HAuCl_4.3H_2O$) was obtained from Sigma-Aldrich Chemical Inc. Clindamycin, streptomycin, flucloxacillin, bacitracin, crystal violate, methylene blue, and nutrient culture media were obtained from the HiMedia Laboratories, Mumbai for the cultivation of *Streptococcus mutans*, *Escherichia coli*, *Pseudomonas aeruginosa* PAO1, *Staphylococcus aureus*, and *C. violaceum* 12472. All other chemicals used were of the highest purity available from commercial sources.

2.2 Preparation of extract

The material of *U. longissima* collected by Dr. R. Bajpai from Govind Wildlife Sanctuary, Uttaranchal, India (Latitude of N 31^0 03' 08.16" & E 78^0 11' 05.50") in October, 2013 and deposited in herbarium of the institute (LWG No. 29343) (Fig. 1A). The material was washed with distilled water to remove the dust particles and then shade-dried to remove the residual moisture. The dried material (10 g) was grinded into coarse size particle and boiled in a 250-mL glass beaker along with

100 mL of sterile distilled water for 12 min. After boiling, the color of the aqueous solution changed from watery to brown (Fig. 1B). The aqueous extract obtained by filtration with Whatman No. 1 filter paper (Pall, USA) was then centrifuged at 2000 rpm for 5 min to remove heavy biomaterials. The *U. longissima* extract (ULE) was used for the development of Uh-Au@Nano-CF using $HAuCl_4$.

2.3 Development of Uh-Au@Nano-CF

In a typical reaction procedure, 10 mL of ULE was challenged with 90 mL of 3mM $HAuCl_4$ solution, with stirring magnetically at 30 ± 0.5 ^{0}C. The color of the mixture of $HAuCl_4$ solution and ULE at 2.5 min of reaction time changed very fast at room temperature after 10 min to a dark purple suspended mixture. This indicated that ULE speeds up the development of Uh-Au@Nano-CF.

2.4 Characterization of Uh-Au@Nano-CF

The developed Uh-Au@Nano-CF was characterized by UV–vis spectrophotometer (Perkin Elmer, USA). X-ray diffraction (XRD) measurement of thoroughly dried thin films of nanoparticles on MiniFlex™ II benchtop XRD system (Rigaku, Tokyo, Japan) operating at 40 kV and a current of 30 mA with Cu Kα radiation (λ = 1.54 A^0) was carried out. The diffracted intensities were recorded from 20^o to 80° 2θ angles. The crystalline size (D) of nanoparticles embedded into the phytochemical(s) of ULE was calculated following the Debye-Scherrer formula:

$$D = 0.9\lambda/\beta\cos\theta$$

Whereas, λ is the wavelength of X-ray, β is the broadening of the diffraction line measured half of its maximum intensity in radians and θ is the Bragg's diffraction angle. The crystalline size of nanoparticles was determined by full width at half maximum (FWHM) value of the (311) peak. Transmission electron microscopy (TEM) of the Uh-Au@Nano-CF was carried out on JEOL 100/120 kV TEM (JEOL, Tokyo, Japan) with an accelerating voltage of ~150 kV. For this, a drop of Uh-

Au@Nano-CF was placed on the carbon coated copper grid and air dried under dark. The obtained TEM microphotographs were converted into an enhanced meta file format [29]. Characterization involved FTIR analysis of the developed Uh-Au@Nano-CF by scanning it in the range from 400-4000 (cm^{-1}) wavenumber. These measurements were carried out on a Perkin Elmer FTIR Spectrum BX (PerkinElmer Life and Analytical Sciences, CT, USA) one instrument in the diffuse reflectance mode at a resolution of 4 cm^{-1} in KBr pellets.

2.5 HPTLC and HPLC analysis

The ULE (5 mg/mL) first was filtered using a 0.22 µm filter paper (Pall, USA) and used for HPTLC analysis. Chromatography was performed on TLC pre-coated silica gel ($60GF_{254}$; Merck) plate. The ULE and reference compound was applied using Camag Linomat V automated TLC applicator with nitrogen flow. Separation of targeted compound(s) was achieved in a Camag twin trough glass chamber using a mobile phase of toluene: ethyl acetate: formic acid (9:1:0.1) till proper separation of bands. The plate was derivatized by anisaldehyde and content of usnic acid was quantified by measuring the band densities of reference compound (usnic acid) and compound detected in the ULE.

RP-HPLC (Shimadzu LC-10A; Kyoto, Japan) equipped with a dual-pump LC-10AT binary system, UV detector SPD-10A (Shimadzu, Kyoto, Japan), and Phenomenex Luna RP, C_{18} column (4.6 x 250 mm) was also employed to complete characterization of ULE. A mobile phase comprising methanol: water: phosphoric acid (80:20:0.9) under isocratic condition was used at the rate of 1 mL/min for the separation of compounds. Identification of compounds was obtained by comparison of the peak at 254 nm with their respective reference compound.

2.6 Preparation of stock culture

A clinical stain of *S. mutans* (MTCC 0497) was obtained from Microbial Type Culture Collection (MTCC), Chandigarh, India and maintained on the slants of Luria-Bertani (LB) agar at 4 ^{0}C. The primary culture of *S. mutans* was prepared from the stock slant into mLB broth medium and incubated at 30 ^{0}C for 24 h under stationary phase. The primary culture (~1 mL) was re-inoculated into 50 mL of fresh LB broth and grown for ~12 h up to mid-log phase (MLP; ~10^5 cfu/mL) at 30 ^{0}C. The all experiments were performed in triplicates using the MLP culture of *S. mutans*.

2.7 Assessment of anti-QS potential of Uh-Au@Nano-CF

2.7.1 Anti-QS activity assay

A standard disk–diffusion assay was used to evaluate the anti-QS activity of Uh-Au@Nano-CF using biomonitor strain of *Chromobacterium violaceum* (ATCC 12472) [17]. This bacterium was cultivated in or on Luria-Bertani (LB) broth (1% tryptone, 0.5% yeast extract, 0.5% NaCl) solidified with 1.2% agar. Five milliliters of molten LB agar (0.25% w/v) was inoculated with 50 µL MLP culture of *C. violaceum* 12472 and then this mixture was immediately poured over the surface of LB agar plates. Various concentrations of Uh-Au@Nano-CF (5, 10 and 15% dilutions) to be tested were pipetted on sterilized paper discs. The plates were incubated overnight at 30 ^{0}C and examined for inhibition of violacein pigment production. The QS inhibition was observed by a colorless and opaque halo zone of inhibition around the disc.

2.7.2 Quantification of violacein production

Quantification of violacein pigment production was carried out as described elsewhere [11]. For extraction of violacein, *C. violaceum* 12472 cells were lysed using 10% sodium dodecyl sulphate (SDS) and solution was incubated at room temperature for 5 min. Then, water saturated n-butanol was

added for fractionating violacein, vortexed, and centrifuged at 13,000 rpm for 10 min. The n-butanol phase was collected and quantified at OD_{585} nm using a UV–Vis spectrophotometer (Thermo-Scientific, USA).

2.7.3 Assessment of virulence factors production in *S. mutans*

The effect of Uh-Au@Nano-CF on degree of glycolytic pH drop by cells was quantified as described earlier [30]. The ATPase activity was examined by adding permeabilized cells of *S. mutans* to 10% toluene followed by series of freezing and thawing as described elsewhere [31]. To determine the lactate dehydrogenase (LDH) activity, cells were incubated at 30 ^{0}C with Tris-HCl and the LDH activity was measured by quantifying the rate of nicotinamide adenine dinucleotide (NADH) oxidation at A_{340} nm [32]. Activity of enolase was measured in permeabilized cells and the results were expressed as enzymatic activity relative to that of the untreated control [31]. Total polysaccharide content was also estimated using Phenol–sulphuric acid method [33]. Chromogenic substrates-based spectrophotometric assay was used for the measurement of protease activity [34]. To determine the gluconase activity, laminarin-dinitrosalicylic acid method was employed [35]. The protein content was measured by the Bradford method using bovine serum albumin (BSA) as the standard [36]. Total carbohydrate was assayed by the method of Dubois et al. [37].

2.7.4 Growth curve assay

The effect of Uh-Au@Nano-CF on growth of *S. mutans* and *C. violaceum* 12472 was determined by monitoring the growth curve [38]. Overnight culture of these bacteria (0.4 OD at A_{600} nm) were inoculated in a 250-mL Erlenmeyer flask containing 50 mL of LB broth and supplemented with 10% solution of the Uh-Au@Nano-CF. The flasks were incubated at 30 ^{0}C under 180 rpm in a rotatory shaker. The cell density was measured by UV–visible spectrophotometry at different time intervals.

2.7.5 Determination of anti-biofilm activity of Uh-Au@Nano-CF

The effect of Uh-Au@Nano-CF on *S. aureus* biofilm development was determined by measuring the biofilm biomass using polyvinyl chloride (PVC) biofilm formation assay [39]. Briefly, MLP culture of *S. aureus* having OD 0.4 at A_{600} nm was added into 1 mL of LB broth medium containing different concentrations of Uh-Au@Nano-CF without agitation for 12 h. The wells were rinsed twice with sterile distilled water to remove the planktonic cells. The surface-adhered cells were stained with 0.4% crystal violate (CV) and 0.2% methylene blue (MB) solutions. After incubation of 2 min at room temperature, excess solution was removed and plates were left for drying and visualized under a light microscope at a magnification of 40x (Nikon Eclipse Ti 100, Tokyo, Japan). For quantification of biofilm inhibition, CV was solubilized by adding 1 mL of 95% ethanol to each well and recorded the absorbance at A_{575} nm by UV–visible spectrophotometer.

Inhibition of biofilm formation was further examined by confocal laser scanning microscopic (CLSM) analysis. Briefly, MLP culture of *S. mutans* was seeded on the cover glasses under LB medium submerged conditions in the absence or presence of Uh-Au@Nano-CF. After incubation of 12 h, biofilms formed on the cover glasses were stained with 20 mM SYTO-9 green fluorescent dye and examined under CLSM (Model LSM510, Germany) and photographed.

2.8 Synergistic action of Uh-Au@Nano-CF with antibiotics

The synergistic action of Uh-Au@Nano-CF with conventional antibiotics was also determined by synergistic assay. Briefly, 1% MLP cultures of test bacteria include *Escherichia coli*, *Pseudomonas aeruginosa* PAO1, *Staphylococcus aureus*, *C. violaceum* 12472, and *S. mutans* (0.4 OD at A_{600} nm) were added to LB broth (1 mL) in 24-well plate and supplemented with antibiotics such as bacitracin (10 µg/mL) for *C. violaceum* 12472, and *S. mutans*, clindamycin (12 µg/mL) for *E. coli*, streptomycin (12 µg/mL) for *P. aeruginosa* PAO1, flucloxacillin (15 µg/mL) for *S. aureus*, and different

concentrations of Uh-Au@Nano-CF. The controls were maintained with respective antibiotics and without Uh-Au@Nano-CF. The plates were incubated at 30 ^{0}C for 24 h and the growth of test bacteria was recorded at A_{600} nm using a UV–visible spectrophotometer.

2.9 Statistical analysis

All experiments were performed in at least triplicates and the data obtained from the experiments were presented as mean ± standard error (SE). The difference between control and test sample was analyzed by Student's *t*-test.

3 Results

3.1 Characterization of Uh-Au@Nano-CF

The reduction of Swarna (Au^{3+}) ions occurred after 10 min of incubation as signified by the development of dark purple colour, indicating the synthesis of Uh-Au@Nano-CF. Time dependent development of colour is shown in Fig. 1C. The appearance of purple colour in the colloidal solution occurs due to localized surface plasmon resonance (LSPR) absorption arising from collective oscillation of free conduction electrons induced by an interacting electromagnetic field [40]. The UV–vis spectrum of the reaction mixture is shown in Fig. 1D. The spectra was recorded by UV-vis spectrophotometer (Perkin Elmer Life and Analytical Sciences, CT, USA) and strong LSPR absorption band (a characteristic peak) was observed at ~550 nm, indicating the synthesis of Swarna nanoparticles as also reported earlier for other biological systems [41, 42]. The control $HAuCl_4$ solution (without ULE) did not display the characteristic peak (data not shown), indicating that reduction of $HAuCl_4$ into Swarna nanoparticles did not occur. The effect of varying $HAuCl_4$ concentrations on nanoparticle synthesis was also examined. A dark purple color was observed when 3.0 mM concentration of the $HAuCl_4$ mixed with 10 mg/mL of ULE (data not shown).

Biomedical application of nanomaterials depends mainly on shape and mono-dispersity which control the optical properties of Swarna nanoparticles. The TEM analysis was used to determine the morphology and size distribution of Uh-Au@Nano-CF. Fig. 1E shows the TEM micrograph of Uh-Au@Nano-CF. The mean particle diameter of Uh-Au@Nano-CF is 14 ± 0.81 nm showed variable morphology, predominantly spherical. The micrograph observation also revealed that the polyphenols rich ULE coated shells on synthesized Swarna nanoparticles resulting in the formation of small and colloidal stable Swarna (Au^0) nanoparticles. Thus, ULE was able to reduce Au^{3+} to form PAu^0 and serve as a stabilizing agent to prevent agglomeration of nanoparticles.

XRD analysis was conducted to confirm the phase of the synthesized of Uh-Au@Nano-CF. Fig. 2A shows the XRD pattern of Uh-Au@Nano-CF synthesized using ULE. The peaks at 2θ values 38.0 °, 44.18° , 64.29°, and 77.19° correspond to (111), (200), (220), and (222) planes of metallic Swarna (Au). The pattern was compared with JCPDS pattern (File No. 04-0784) and was indexed to cubic of Swarna nanoparticles. The average size of Swarna nanoparticles was calculated to be ~28 nm using the Debye–Scherrer's formula by determining the FWHM of the (111) Bragg's reflection [43, 44].

FTIR analysis was used to identify the possible bio-reducing biomolecules in the ULE. The spectra showed strong bands at (1351 and 1450), (1617 and 1609), (1701 and 1721), (2928 and 2952), and (3380 and 3395) cm^{-1}, respectively (Fig. 2B-a). The intense vibration peak at 3380 cm^{-1} appeared due to the stretching vibration of the aliphatic and aromatic OH groups. The broadness of this band shows the intermolecular hydrogen bonding among the OH groups. The peaks in the range from 1609 to 1400 cm^{-1} were due to presence of aromatic rings of phytochemicals in the ULE. The vibration peak at 1351 cm^{-1} was due to the in-plane bending of the OH groups.

In FTIR spectrum of the Uh-Au@Nano-CF, the stretching vibration due to the aliphatic and aromatic OH groups became narrower and shifted to 3395 cm^{-1} due to weakening of the

intermolecular H-bonding (Fig. 3B-b). The in-plane bending frequency of OH group became much weaker in case of Uh-Au@Nano-CF. These FTIR results clearly showed that the involvement of ULE's polyphenols in the synthesis of Swarna nanoparticles and their encapsulation through interaction with OH group of phytochemicals which present in ULE. Next we examined the stability of synthesized Uh-Au@Nano-CF (15% solution) in bacterial culture medium (LB broth) at 30 ^{0}C through the change in LSPR characteristics using UV-vis spectrophotometer (Fig. 2C). No significant changes such as absorbance and agglomeration were observed, suggesting encapsulation of nanoparticles could be responsible for their prolonged stability [21, 38].

3.2 Characterization of phytochemical(s) in ULE

The brown coloured ULE was obtained by boiling of plant material in distilled water. Characterization of phytochemical of ULE is given in Fig. 3A-D. The HPTLC analytical study of the ULE has resulted in the identification of polyphenolic usnic acid at R_f 0.79 representing 1.97% of the total extract. However, other bands were also detected, suggesting that ULE contains other compounds.

More characterization of phytochemicals present in the ULE was further done by RP-HPLC Separation of compounds was achieved with methanol: water: phosphoric acid (80:20:0.9) as a mobile phase under isocratic condition. In addition to usnic acid, the HPLC fingerprinting also showed the presence of other phytochemicals such as orcinol, apigenin, and arabitol (Fig. 3E).

3.3 Mechanism of Uh-Au@Nano-CF development

The mechanism involved in the development of Swarna-based colloidal nano-formulation is still unclear. The overall mechanism for development of Uh-Au@Nano-CF using ULE is schematically presented in an equation 1. The ULE mainly consists of polyphenolic compounds, predominantly usnic acid. It has been reported that the water extract of *U. longissima* and its usnic acid component

exhibit strong antioxidant activity under *in-vitro* and *in-vivo* studies [9]. Herein, the reduction of $HAuCl_4$ occurs due to antioxidant activity (transfer of electrons) from the polyphenols of ULE to the Swarna ions, resulting in the development of Uh-Au@Nano-CF as follows:

$$HAuCl_4 + \text{Polyphenols (OH)} \rightarrow Au^0 + \text{Polyphenols } (^{+\bullet}\text{OH}) + H^+ + 4Cl^- \quad \text{……(equation 1)}$$

This antioxidant polyphenolic compounds are mainly responsible for the reduction of Swarna (Au^{3+} in $HAuCl_4$) to Au^0 (Swarna nanoparticle). The direct participation of usnic acid and other antioxidant polyphenols in the synthesis of Swarna nanoparticles has been already reported [45].

3.4 Anti-QS activity of Uh-Au@Nano-CF

Anti-QS activity of Uh-Au@Nano-CF was evaluated using the bioindicator strain *C. violaceum* 12472. In this bacterium, production of a purple pigment, violacein, is under QS-control [10]. Inhibition of purple pigment in *C. violaceum* 12472 is indicative of QS attenuation by Uh-Au@Nano-CF (Fig. 4A). An opaque and halo zone of inhibition around the disc was examined by Uh-Au@Nano-CF. It was associated with the inhibition of QS, not due to inhibition of bacterium growth. Strong QS inhibition was observed, when applied 15% solution of Uh-Au@Nano-CF. Control discs having sterilized distilled water, gentamycine (12 µg/mL), and halogenated furanone (5 µg/mL) were included. As expected, a zone of growth inhibition was observed with gentamycine, a zone of QS-attenuation was seen with the furanone, and no inhibition was apparent with water (Fig. 4A).

Quantitative inhibitory potential of Uh-Au@Nano-CF on violacein production was also determined spectrophotometrically. Fig. 4B shows the increasing concentrations of Uh-Au@Nano-CF led to an incremental reduction in the violacein production in *C. violaceum* 12472. It was also confirmed whether Uh-Au@Nano-CF at 15% concentration inhibits the growth of CV026 and the data revealed non-cidal effect of Uh-Au@Nano-CF (Fig. S1). Free Swarna nano-colloidal solution (15%) and free ULE (0.1g/mL) were also subjected to determine their anti-QS activity. Interestingly, both

362 revealed very weak anti-QS activity, confirmed by disc diffusion (Fig. S2A and B) and violacein
363 pigment quantification (Fig. S2C and D) assays.
364 .
365 **3.5 Effect of Uh-Au@Nano-CF on extracellularly secreted virulence factors**
366 The glycolytic acid production by *S. mutans* found to be significantly reduced in the initial and final
367 rate of the pH by Uh-Au@Nano-CF (Fig. 5A). The onset pH 7.2 was decreased to 3.7 after 3 h of
368 incubation in the untreated control. The most significant change from acidic to near alkaline pH after
369 48 h of incubation was determined in 15% Uh-Au@Nano-CF treated culture, where the acidic pH 3.7
370 was increased to 7.0. This inhibitory effect of the Uh-Au@Nano-CF may be due to the inhibition of
371 bacterial QS signaling pathway.
372 It has been reported that ATPase controls acid tolerance of *S. mutans* by regulating pH
373 gradient across the membrane [46]. It is evident from the data recorded, that the exposure of 5-15%
374 solutions of Uh-Au@Nano-CF showed remarkable reduction in ATPase activity ranged from 9.7 to
375 74.6% as compared to untreated controls (Fig. 5B). Therefore, the inhibition of ATPase activity may
376 contribute to increased acidity in cytoplasm resulting in decreased acid adaptation [47]. Meanwhile,
377 alkaline pH of cytoplasm is important for normal functioning of a series of enzymes involved in
378 physiological processes, while its acidification could lead to potential mortal effect on *S. mutans*.
379 Besides, a similar pattern of decline was also examined for LDH activity as shown in Fig. 5C.
380 The Uh-Au@Nano-CF at 15% dilution was found to decrease the activity of LDH by 51.9%. Fig. 5D
381 shows the inhibitory effect of Uh-Au@Nano-CF on enolase activity. Treatment of 15% Uh-
382 Au@Nano-CF caused 49.4% reduction in the activity of enolase, when compared to untreated control.
383 The Uh-Au@Nano-CF suppressed the total polysaccharide levels ranged from 7.8 to 48.5% in a
384 concentration dependent manner (Fig. 5E). Figures 5F and G show substantial decline in the
385 production of hydrolytic enzymes such as protease and glucosidase, respectively. The Uh-Au@Nano-

CF reduced the activity of protease by 65.4%, whereas glucosidase activity by 55.2%, when compared to their respective untreated controls. Moreover, the protein content for samples treated with 15% solution of Uh-Au@Nano-CF was 2.7 mg/mL, while for control sample was 3.4 mg/mL (Fig. S3). In addition, a weak inhibitory effects of free Swarna nanoparticles (15%) and free ULE (0.1 mg/mL) on the secretion of these virulence factors were observed (data not shown). Hence, our investigation confirms that the inhibition of virulence factors production in *S. mutans* is a net result of QS inhibition by Uh-Au@Nano-CF.

3.6 Anti-biofilm activity of Uh-Au@Nano-CF

S. mutans forms biofilm, a QS controlled phenomenon, in which cells are organized into layers and enmeshed in a matrix of mucoid polysaccharides [48, 49]. A switch to the biofilm mode of growth confers increased antibiotic resistance and creates a considerably more severe infection in the skin and teeth of patients with dental carries. We sought to examine weather Uh-Au@Nano-CF could inhibit biofilm formation in *S. mutans*. Direct observations by microscopy of biofilms could provide valuable information on biofilms organization; therefore light microscopy analysis was performed. We treated the cells with Uh-Au@Nano-CF and examined the biofilm formation using CV, SYTO-9, and MB staining techniques. A dark staining of CV due to thick coating of biofilms was examined in controls. However a visible reduction in numbers of microcolonies was examined in the biofilms of *S. mutans* treated with Uh-Au@Nano-CF (Fig. 6A). Moreover, Uh-Au@Nano-CF deteriorated the architecture of the biofilm too, as it was more evident from CLSM analysis (Fig. 6B) as well as MB staining (Fig. 6C). The anti-biofilm activity of Uh-Au@Nano-CF against using a standard quantitative microtiter dish biofilm formation assay and showed a concentration-dependent reduction in biofilm formation of *S. mutans*. A significant inhibition was examined which ranged from 24.92% to 94.17%, when cells were exposed to 5-15% solutions of Uh-Au@Nano-CF (Fig. 6D).

We next investigated whether Uh-Au@Nano-CF alters biochemical composition of *S. mutans* biofilm matrix. Carbohydrates are main components of bacterial biofilm matrix. It forms a three dimensional, gel-like, highly resistant and locally charged environment in which the cells are largely immobilized. Total carbohydrate content was found to decrease in Uh-Au@Nano-CF-treated biofilms of *S. mutans* (Fig. S4). The effect of Uh-Au@Nano-CF on *S. mutans* growth using growth curve analysis was also examined. The treated and untreated cultures of *S. mutans* were grown to early stationary phase and the obtained data revealed that the cell densities did not differ between untreated control and Uh-Au@Nano-CF treated cultures (Fig. 6E). The results indicate that inhibition of QS and biofilm formation by Uh-Au@Nano-CF was not associated with its cidal effect. Our results are very well corroborated with the findings reported earlier [50-54]. Free Swarna nanoparticles and free ULE exhibited low anti-biofilm activity, compared to Au@Nano-CF (Fig. S5A and B). Usnic acid from the *U. longissima* is known for anti-biofilm by inhibiting biofilm formation or by eradicating preformed biofilms at higher concentration [55]. Several studies have reported the synergistic effect of biogenic metal nanoparticles and plant extracts on the biofilm of clinical isolates of bacteria [56, 57].

3.7 Synergistic activity of Uh-Au@Nano-CF with antibiotics

It is well documented that increased sensitivity towards antibiotics depends on the process of QS. Most of the bacterial pathogens are generally resistant or less sensitive towards antibiotics. In the present investigation, we exposed the *Escherichia coli* to clindamycin, *Pseudomonas aeruginosa* PAO1 to streptomycin, *Staphylococcus aureus* to flucloxacillin, *C. violaceum* 12472, and *S. mutans* to bacitracin. The enhanced susceptibility of all test bacterial pathogens towards respective antibiotics was examined in the presence of Uh-Au@Nano-CF. The obtained results revealed that increasing concentration of Uh-Au@Nano-CF (5–15%) with antibiotics enhanced the susceptibility of test pathogens towards respective antibiotics (Table 1).

4 Discussion

The virulence of *S. mutans* is owed to its capacity to degrade host tissue with production of organic acid, enzymes and toxins, and to avoid antibiotic attack by forming biofilms. Biofilm formation and the virulence factors examined in this study are under QS control [48]. Thus, the Uh-Au@Nano-CF was evaluated for its ability to interfere with QS-dependent production of *S. mutans* virulence factors acidogenesis, enolase, protease, LDH, glucosidase, and polysaccharide production. In addition, we examined the ability of Uh-Au@Nano-CF to inhibit biofilm formation.

Antibiotic-based antimicrobial therapies which suppress the growth of certain bacteria have the drawback of developing resistance against the drugs. QS is a key regulator of virulence factors production in *S. mutans* and other medically relevant bacteria [16, 48, 58]. In this sense, inhibiting only secretion of virulence factors of bacteria without affecting their growth, seems to be an attractive alternative that would reduce the risk of selecting resistant bacteria as well as could be an appealing approach for the prevention of *S. mutans* persistence and pathogenesis. The potential of herbo-metallo colloidal nano-formulation to interfere with QS of bacteria is new and it has not been previously described by other authors. Therefore, the purpose of the present study is to explore the newer pharmacological activity of the Uh-Au@Nano-CF. It was interesting to observe that the Uh-Au@Nano-CF was able to decrease acid production and activities of ATPase, LDH, enolase, protease and glucosidase. Acid production and acid tolerance are QS-regulated vital virulence factors of *S. mutans* [47]. Even in highly acidic conditions, it emerges out to be most prevalent inhabitant of cariogenic plaque. Hence, stress tolerance plays a key role in its pathogenesis. Hasan and colleagues reported that the cariostatic effect can be controlled by regulating bacterial acidogenesis and the enzyme associated with the glycolysing systems [59]. ATPase is known to regulate acid tolerance in *S. mutans* via maintenance of pH gradient across the membrane [46]. LDH is well documented for lactic

457 acid production and promotes pathogenicity of *S. mutans* [32]. The suppression of LDH activity induces
458 NAD^+/NADH imbalance and accumulation of glycolytic intermediates in the cell, which act as toxin
459 for *S. mutans* [32, 47]. Hence, it would result in reduced alkali condition in cytoplasm and inhibited
460 glycolysis with reduced ATP pools, leading to compromised adaptation to environmental stress and
461 decreased cellular functions, thereby increasing cell death by the antimicrobial agents. Enolase, a key
462 enzyme of glycolysis which regulates the formation of phosphoenolpyruvate [60]. Therefore, the
463 suppression of enolase activity could not only result in reduced glycolysis but could also decrease the
464 downstream production of phosphoenolpyruvate, resulting in inhibited acid production. Protease and
465 glucosidase activities are believed to play a major role in pathogenesis via host tissue degradation.
466 This confirms the inhibitory effect of Uh-Au@Nano-CF on secretion of virulence factors which was
467 associated with attenuation of QS signaling in *S. mutans*.

468 *U. longissima* is rich in usnic acid, and its antimicrobial activity has been well described [28].
469 The ethnobotanical use of this lichen in herbal tooth powder is also known. On the other hand,
470 antimicrobial potential of Swarna nanoparticles has been previously reported by other researchers [61,
471 62]. It would therefore be plausible that antimicrobial Swarna nanoparticles and usnic acid present in
472 Uh-Au@Nano-CF could be related to the inhibition of *S. mutans* virulence factors.

473 Biofilm formation in *S. mutans* is suggested to be positively controlled by QS signaling. Since,
474 Swarna nanoparticles and usnic acid demonstrated inhibition of biofilm formation in certain bacteria;
475 we further hypothesized that our developed Uh-Au@Nano-CF may also influence the biofilm
476 formation in *S. mutans*. Indeed, the Uh-Au@Nano-CF showed potent anti-biofilm activity, inhibiting
477 biofilm formation. Disruption of the QS system using usnic acid isolated from *Usnia* species has also
478 been shown to inhibit biofilm formation [28]. Earlier studies carried out with Swarna nanoparticles
479 revealed a qualitative modification in biofilm morphology and a reduction in thickness [24]. Moreover,

480 *S. mutans* growth was not affected by Uh-Au@Nano-CF treatment under experimental conditions.
481 Together, these results seem to suggest that the Uh-Au@Nano-CF exhibits anti-biofilm activity in
482 non-growth inhibitory fashion and plausibly in QS dependent manner. But, biofilm formation is a
483 complex multi-factorial process, which is controlled by a combination of environment and genotype.
484 Therefore, the possibility of Uh-Au@Nano-CF acting via some other factors cannot be negated.

485 Recently our group has reported that enhanced sensitivity towards antibiotics relies on the
486 process of QS [10]. *S. mutans* is generally resistant or less sensitive to its respective antibiotics. In this
487 study, Uh-Au@Nano-CF was found to enhance the susceptibility of *S. mutans* towards its respective
488 antibiotics. Similar to the reports of Hentzer and Givskov, wherein halogenated furanone compounds
489 act synergistically with tobramycin to destruct *P. aeruginosa* biofilms [63]. Similarly, green fruit extract
490 of *Lagerstroemia speciosa* found to enhance the susceptibility of *P. aeruginosa* PAO1 towards
491 tobramycin (Singh et al., 2012). Given the widespread occurrence of QS systems, it has been showed
492 that interfering with the cell-to-cell communication system may pave way to prevent the development
493 of biofilm formation and subsequent tooth infections.

494

495 ## 5 Conclusion

496 This study presents a novel antimicrobial herbo-Swarna colloidal nano-formulation and demonstrates
497 its new biomedical use for combating infections through attenuation of virulence of *S. mutans* rather
498 than viability. Opening the possibility of a new anti-pathogenic effect through interference with the
499 bacterial QS, the anti-virulence ability of Uh-Au@Nano-CF may be related to the synergistic effect of
500 Swarna nanoparticles and polyphenols particularly usnic acid of *U. longissima* that could inhibit QS
501 systems of *S. mutans*. Further studies should be performed to validate the results and to realize the
502 application of this anti-QS colloidal nano-formulation for combating microbial infections caused by *S.*
503 *mutans*.

Funding

The study was financially supported by the Council of Scientific & Industrial Research (BSC-0106 & OLP-089) and Department of Science & Technology (GAP 3325), New Delhi, India.

Disclosure statement

The authors declare that they have no competing interests.

Acknowledgments

The authors would like to thank the CSIR, India for the financial support. Authors are grateful to Dr. C.S. Nautiyal, Director National Botanical Research Institute, Lucknow, India and Prof. A.H. Naqvi, Director Center of Nanotechnology, Aligarh Muslim University, Aligarh, India for providing research facilities. Dr. Braj R. Singh is also thankful to the CSIR, India for awarding Pool Scientists Scheme (13(8595-A) 2012-Pool).

References

1. S. Nagarajan, K. Sivaji, S. Krishnaswamy, B. Pemiah, K. S. Rajan, U. M. Krishnan and S. Sethuraman, *J. Ethnopharmacol.*, 2014, **151**, 1-11.
2. G. Kumar and Y. K. Gupta, *Ayu*, 2012, 33, 569-575.
3. A. Kumar, A. G. C. Nair, A. V. R. Reddy and A. N. Garg, *Biol. Trace Elem. Res.*, 2006, **109**, 231-254.
4. S. Khedekar, B. J. Patgiri, B. Ravishankar and P. K. Prajapati, *Ayu*, 2011, 32, 109-115.
5. S. Das, M. C. Das and R. Paul, *Ayu.*, 2012, **33**, 365-367.
6. S. Mohaptra and C. B. Jha, *Int. J. Ayurveda Res.*, 2010, **1**, 82-86.
7. S. Kocer, S. Urus, A. Cakir, M. Gulluce, M. Digrak, Y. Alan, A. Aslan, M. Tumer, M. Karadayi, C. Kazaz and H. Dal, *Dalton Trans.*, 2014, **43**, 6148-6164.
8. M. I. Choudhary, Azizuddin, S. Jalil and R. Atta ur, *Phytochemistry*, 2005, **66**, 2346-2350.
9. M. Halici, F. Odabasoglu, H. Suleyman, A. Cakir, A. Aslan and Y. Bayir, *Phytomedicine*, 2005, **12**, 656-662.
10. B. N. Singh, H. B. Singh, A. Singh, B. R. Singh, A. Mishra and C. S. Nautiyal, *Microbiology*, 2012, **158**, 529-538.
11. B. N. Singh, B. R. Singh, R. L. Singh, D. Prakash, R. Dhakarey, G. Upadhyay and H. B. Singh, *Food Chem. Toxicol.*, 2009, **47**, 1109-1116.
12. A. L. Adonizio, K. Downum, B. C. Bennett and K. Mathee, *J. Ethnopharmacol.*, 2006, **105**, 427-435.
13. R. Naidoo, M. Patel, Z. Gulube and I. Fenyvesi, *J. Ethnopharmacol.*, 2012, **144**, 171-174.
14. J. Limsong, E. Benjavongkulchai and J. Kuvatanasuchati, *J. Ethnopharmacol.*, 2004, **92**, 281-289.
15. D. H. Lee, B. R. Seo, H. Y. Kim, G. C. Gum, H. H. Yu, H. K. You, T. H. Kang and Y. O. You, *J. Ethnopharmacol.*, 2011, **137**, 979-984.
16. Z. T. Wen, D. Yates, S. J. Ahn and R. A. Burne, *BMC Microbiol.*, 2010, **10**, 111.
17. B. N. Singh, B. R. Singh, R. L. Singh, D. Prakash, B. K. Sarma and H. B. Singh, *Food Chem. Toxicol.*, 2009, **47**, 778-786.
18. J. C. Taganna, J. P. Quanico, R. M. Perono, E. C. Amor and W. L. Rivera, *J. Ethnopharmacol.*, 2011, 134, 865-871.
19. D. Mothey, B. A. Buttaro and P. J. Piggot, *FEMS Microbiol. Lett.*, 2014, **350**, 161-167.
20. S. Hahnel, D. S. Wastl, S. Schneider-Feyrer, F. J. Giessibl, E. Brambilla, G. Cazzaniga and A. Ionescu, *J. Adhes. Dent.*, 2014, **16**, 313-21.
21. B. R. Singh, B. N. Singh, W. Khan, H. B. Singh and A. H. Naqvi, *Biomaterials*, 2012, **33**, 5753-5767.
22. B. N. Singh, A. K. Rawat, W. Khan, A. H. Naqvi and B. R. Singh, *PLoS One*, 2014, **9**, e106937.
23. G. R. Salunke, S. Ghosh, R. J. Santosh Kumar, S. Khade, P. Vashisth, T. Kale, S. Chopade, V. Pruthi, G. Kundu, J. R. Bellare and B. A. Chopade, *Int. J. Nanomed.*, 2014, **9**, 2635-2653.
24. M. B. Sathyanarayanan, R. Balachandranath, Y. Genji Srinivasulu, S. K. Kannaiyan and G. Subbiahdoss, *ISRN Microbiol.*, 2013, **2013**, 272086.
25. S. N. Sawant, V. Selvaraj, V. Prabhawathi and M. Doble, *PLoS One*, 2013, **8**, e63311.
26. S. Khan, F. Alam, A. Azam and A. U. Khan, *Int. J. Nanomed.*, 2012, **7**, 3245-3257.
27. A. M. Grumezescu, C. Saviuc, M. C. Chifiriuc, R. Hristu, D. E. Mihaiescu, P. Balaure, G. Stanciu and V. Lazar, *IEEE Trans Nanobiosci.*, 2011, **10**, 269-274.

28. I. Francolini, P. Norris, A. Piozzi, G. Donelli and P. Stoodley, *Antimicrob. Agents Chemother.*, 2004, **48**, 4360-4365.
29. J. A. Khan, M. Qasim, B. R. Singh, S. Singh, M. Shoeb, W. Khan, D. Das and A. H. Naqvi, *Spectrochim. Acta Part A: Mol. Biomol. Spectro.*, 2013, **109**, 313-321.
30. S. H. Ban, J. E. Kim, S. Pandit and J. G. Jeon, *Molecules*, 2012, **17**, 9231-9244.
31. W. A. Belli, D. H. Buckley and R. E. Marquis, *Can. J. Microbiol.*, 1995, **41**, 785-791.
32. S. Hasan, K. Singh, M. Danisuddin, P. K. Verma and A. U. Khan, *PLoS One*, 2014, **9**, e91736.
33. M. Bergamaschi, *Sperimentale*, 1959, **109**, 347-358.
34. K. Nakashima, T. Maruyama, N. Kamiya and M. Goto, *Anal. Biochem.*, 2008, **374**, 285-290.
35. B. N. Singh, A. Singh, B. R. Singh and H. B. Singh, *J. Appl. Microbiol.*, 2013, **116**, 654-666.
36. J. B. Hammond and N. J. Kruger, *Methods Mol. Biol.*, 1988, **3**, 25-32.
37. K. P. Dubois and A. B. Raymund, *Q Prog Rep United States Air Force Radiat Lab Univ Chic*, 1960, **37**, 32-37.
38. M. Shoeb, B. R. Singh, J. A. Khan, W. Khan, B. N. Singh, H. B. Singh and A. H. Naqvi, *Adv. Nat. Sci.: Nanosci. Nanotechnol.*, 2013, **4**, 035015.
39. S. J. Ahn, Z. T. Wen, L. J. Brady and R. A. Burne, *Infect. Immun.*, 2008, **76**, 4259-4268.
40. N. Vasimalai and S. A. John, *J. Mat. Chem. A*, 2013, **1**, 4475-4482.
41. J. Patel, L. Němcová, P. Maguire, W. G. Graham and D. Mariotti, *Nanotechnology*, 2013, **24**, 245604.
42. D. Correa-Llanten, S. Munoz-Ibacache, M. Castro, P. Munoz and J. Blamey, *Microbial. Cell Factories*, 2013, **12**, 75.
43. S. S. Shankar, A. Ahmad, R. Pasricha and M. Sastry, *Journal of Materials Chemistry*, 2003, **13**, 1822-1826.
44. V. S. Suvith and D. Philip, *Spectrochimica Acta Part A: Molecular and Biomolecular Spectroscopy*, 2014, **118**, 526-532.
45. T. Panda and K. Deepa, *J. Nanosci. Nanotechnol.*, 2011, **11**, 10279-10294.
46. I. R. Hamilton and N. D. Buckley, *Oral Microbiol. Immunol.*, 1991, **6**, 65-71.
47. H. K. Kuramitsu, *Crit. Rev. Oral Biol. Med.*, 1993, **4**, 159-176.
48. D. Senadheera and D. Cvitkovitch, in *Bacterial Signal Transduction: Networks and Drug Targets*, ed. R. Utsumi, Springer New York, 2008, vol. **631**, ch. 12, pp. 178-188.
49. Y.-H. Li and X. Tian, *Sensors*, 2012, **12**, 2519-2538.
50. E. Boisselier and D. Astruc, *Chem Soc Rev*, 2009, **38**, 1759-1782.
51. M. M. Khan, S. Kalathil, T. H. Han, J. Lee and M. H. Cho, *J. Nanosci. Nanotechnol.*, 2013, **13**, 6079-6085.
52. A. R. Stojak, T. Raftery, S. J. Klaine and T. L. McNealy, *Nanotoxicology*, 2011, **5**, 730-742.
53. M. B. Sathyanarayanan, R. Balachandranath, Y. Genji Srinivasulu, S. K. Kannaiyan and G. Subbiahdoss, *ISRN Microbiology*, 2013, **2013**, 5.
54. T. Read, R. V. Olkhov and A. M. Shaw, *Phy. Chem. Chem. Phy.*, 2013, **15**, 6122-6127.
55. M. C. Chifiriuc, L. M. Ditu, E. Oprea, S. Litescu, M. Bucur, L. Marutescu, G. Enache, C. Saviuc, M. Burlibasa, T. Traistaru, G. Tanase and V. Lazar, *Roum Arch. Microbiol. Immunol.*, 2009, **68**, 215-222.
56. S. Gurunathan, J. W. Han, D. N. Kwon and J. H. Kim, *Nanoscale Res. Lett.*, 2014, **9**, 373.
57. A. Nithya Deva Krupa and V. Raghavan, *Bioinorg. Chem. Appl.*, 2014, **2014**, 949538.

58. J. Singh, P. Khalichi, D. G. Cvitkovitch and J. P. Santerre, *J. Biomed. Mater. Res. A*, 2009, **88**, 551-560.
59. S. Hasan, M. Danishuddin, M. Adil, K. Singh, P. K. Verma and A. U. Khan, *PLoS One*, 2012, **7**, e40319.
60. P. W. Postma, J. W. Lengeler and G. R. Jacobson, *Microbiol. Rev.*, 1993, **57**, 543-594.
61. J. F. Hernandez-Sierra, F. Ruiz, D. C. Pena, F. Martinez-Gutierrez, A. E. Martinez, J. Guillen Ade, H. Tapia-Perez and G. M. Castanon, *Nanomedicine*, 2008, **4**, 237-240.
62. E. Lima, R. Guerra, V. Lara and A. Guzman, *Chem Cent J*, 2013, **7**, 11.
63. M. Hentzer, H. Wu, J. B. Andersen, K. Riedel, T. B. Rasmussen, N. Bagge, N. Kumar, M. A. Schembri, Z. Song, P. Kristoffersen, M. Manefield, J. W. Costerton, S. Molin, L. Eberl, P. Steinberg, S. Kjelleberg, N. Hoiby and M. Givskov, *EMBO J.*, 2003, **22**, 3803-3815.

Legends of figure

Fig. 1 Plant material of *U. longissima* (A) and its aqueous extract (B). (C) Illustrates the development of Uh-Au@Nano-CF is completed in 10 min. (D) UV-visible spectrum of developed Swarna nanoparticles at different time intervals showed peak at 550 nm. (E) TEM image of Swarna nanoparticles synthesized by ULE.

Fig. 2 (A) Representative XRD profile of synthesized Swarna nanoparticles. (B) FTIR spectrum of ULE and Swarna nanoparticles shows possible interaction between the nanoparticles and phyto-molecules present in ULE. (C) Prolonged stability of Swarna nanoparticles at room temperature confirms encapsulation of nanoparticle by phyto-molecules of ULE.

Fig. 3 HPTLC and HPLC fingerprinting of ULE. After derivatization of TLC plate pre-coated with silica gel ($60GF_{254}$) by anisaldehyde, the plate was photographed under UV at 254 nm (A) and 366 nm (B). Then plate was scanned at 280 nm for detection of reference compound (C) and compounds present in ULE (D) using *CAMAG* HPTLC instrument. (E) RP-HPLC chromatogram of ULE shows the presence of orcinol, arabitol, apigenin, and usnic acid. R, reference compound; S, plant extract (ULE).

Fig. 4 Anti-QS activity of Uh-Au@Nano-CF using *C. violaceum* 12472, a biomonitor strain. (A) A white halo zone/or inhibition of violacein production around the disc indicates an anti-QS activity. Control discs containing sterilized distilled water, gentamycin (12 µg/mL), and halogenated furanone (5 µg/mL). (B) Quantification of violacein production in *C. violaceum* 12472 treated with indicated dilutions of Uh-Au@Nano-CF for 48 h. Data are mean and SE (n = 8).

Fig. 5 Impact of Uh-Au@Nano-CF on extracellularly secreted virulence factors in *S. mutans*. Cells were exposure to indicated times and dilutions of Uh-Au@Nano-CF and examined the inhibitory effect on (A) pH drop, (B) ATPase activity, (C) LDH activity, (D) enolase activity,

655 (E) polysaccharide synthesis, (F) protease activity, and (G) gluconase activity in *S. mutans*.
656 Data are means and SE (n = 6).*Significant difference compared with the untreated control
657 ($P < 0.01$).

658 **Fig. 6** Effect of Uh-Au@Nano-CF on *S. mutans* biofilm development. Bacterial biofilms
659 were grown in the absence or presence of indicated dilutions of Uh-Au@Nano-CF. Images of
660 (A) CV-stained light microscope, (B) CLSM, and (C) MB-stained light microscope. (D)
661 Quantitative analysis of anti-biofilm activity of Uh-Au@Nano-CF. (E) Cells were grown in
662 the absence and presence of 15% Uh-Au@Nano-CF. Samples were taken at indicated time
663 intervals and recorded the growth of *S. mutans* at OD_{600} nm. Data are means and SE (n = 6).

664
665
666
667
668
669
670
671
672
673
674
675

676 **TABLE**

677 Table 1. Synergistic action of Uh-Au@Nano-CF with antibiotics

678

Bacterial pathogen	Antibiotic	% Growth reduction (Antibiotic alone)	% Growth reduction (Uh-Au@Nano-CF +Antibiotic)		
			5%	10%	15%
E. coli	Clindamycin (12 µg/mL)	51.62 ± 2.11	52.84 ± 1.83	67.92 ± 3.17	82.16 ± 4.76
P. aeruginosa PAO1	Streptomycin (12 µg/mL)	47.81 ± 3.49	48.11 ± 3.27	55.64 ± 2.19	76.83 ± 2.61
C. violaceum 12472	Bacitracin (10 µg/mL)	41.83 ± 2.57	43.61 ± 3.52	63.41 ± 3.66	88.48 ± 5.51
S. mutans	Bacitracin (10 µg/mL)	51.72 ± 4.16	52.38 ± 3.86	65.71 ± 3.18	82.81 ± 3.81
S. aureus	Flucloxacillin (15 µg/mL)	42.81 ± 2.73	43.72 ± 2.63	65.83 ± 63.2	91.26 ± 6.82

679

680 Each value is expressed as means ± SD (n = 6)

681

(A)

(B)

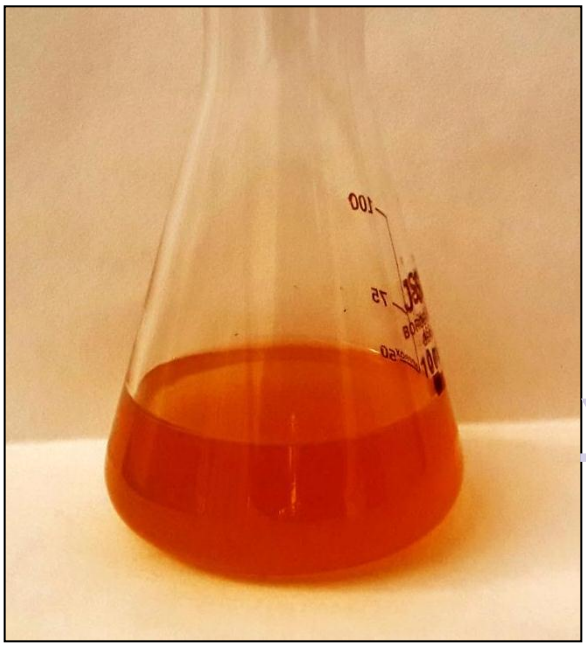

(C)

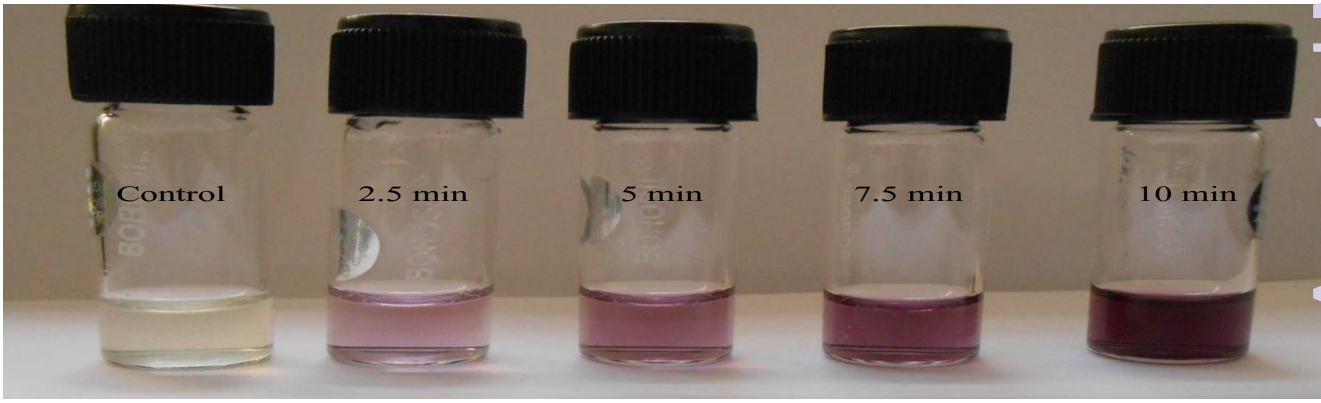

(D)

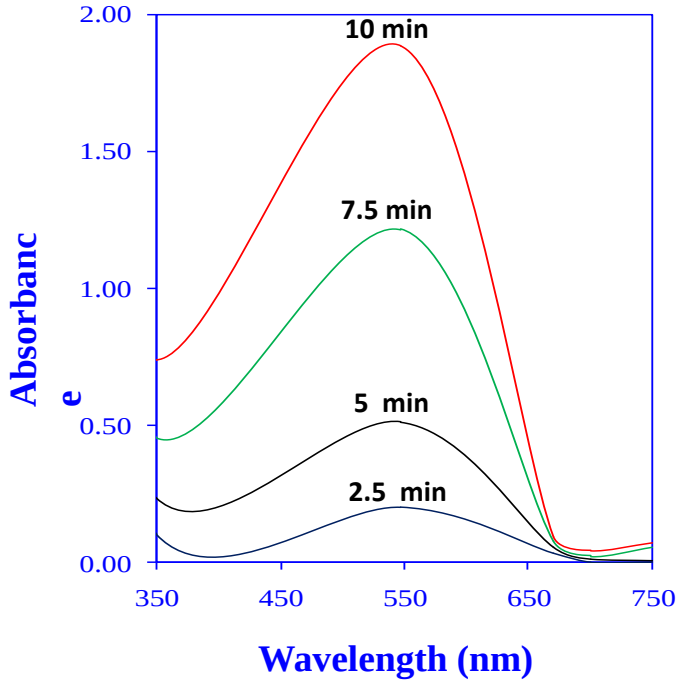

(E)

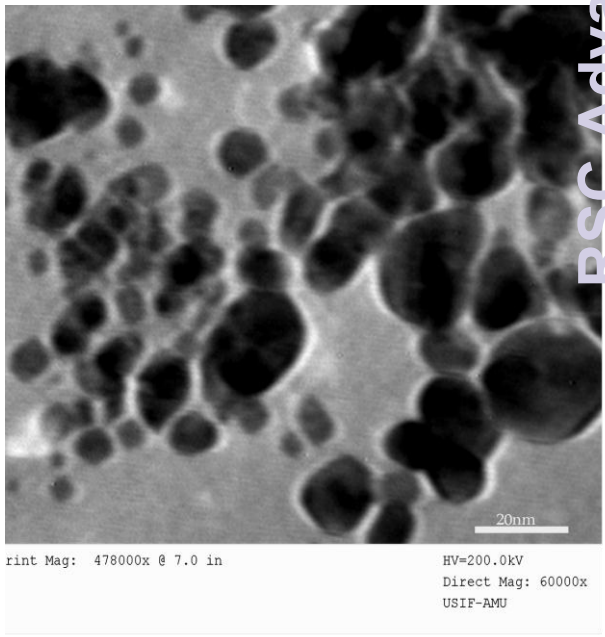

Fig. 2

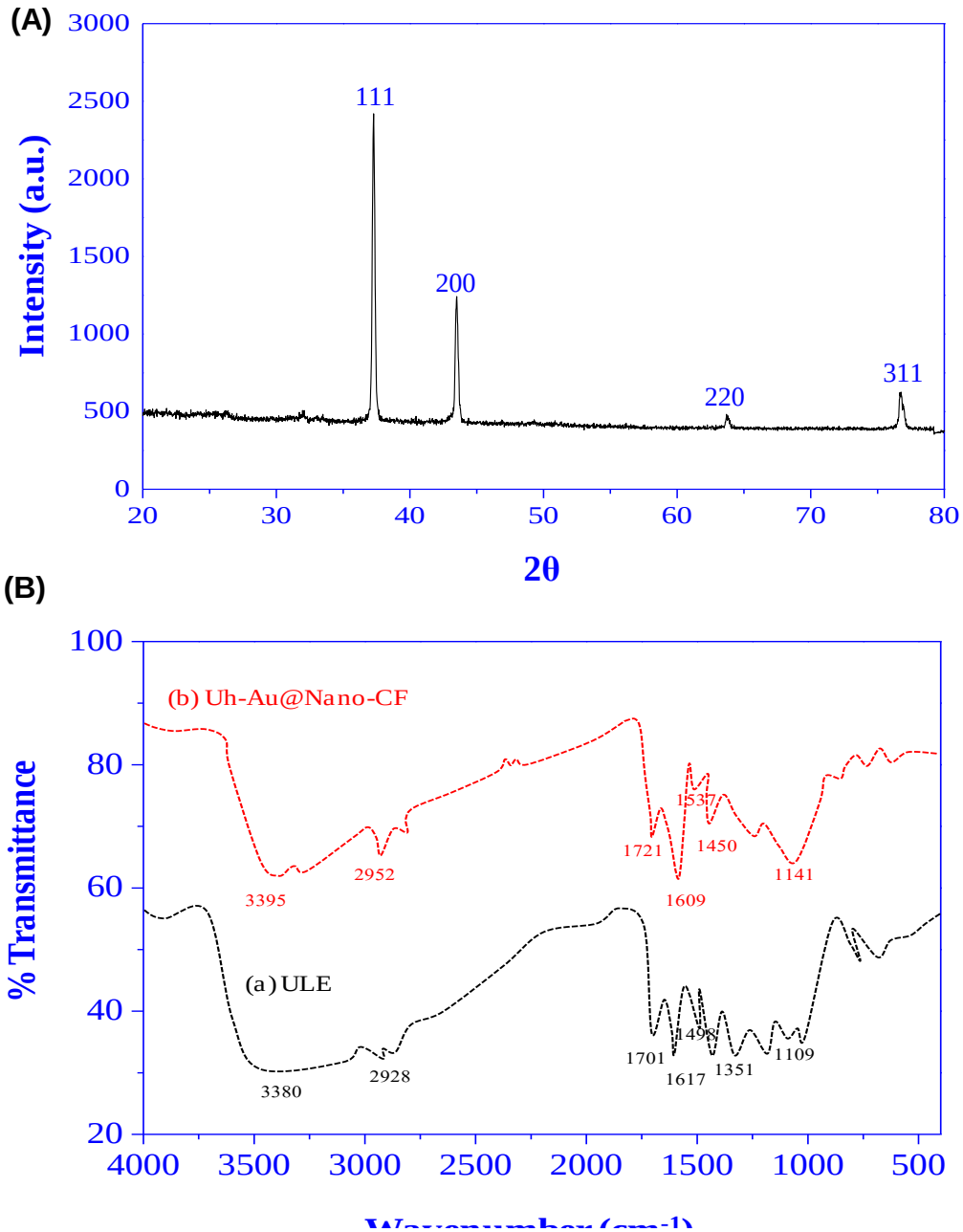

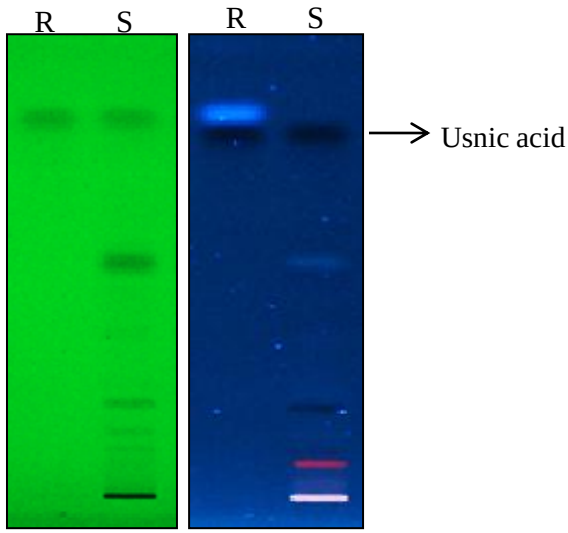

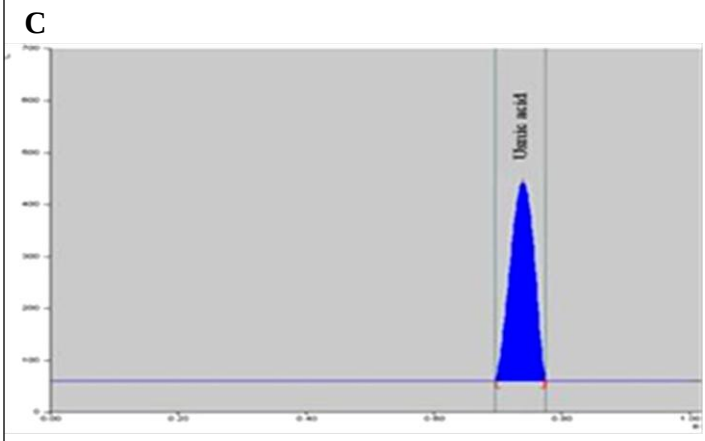

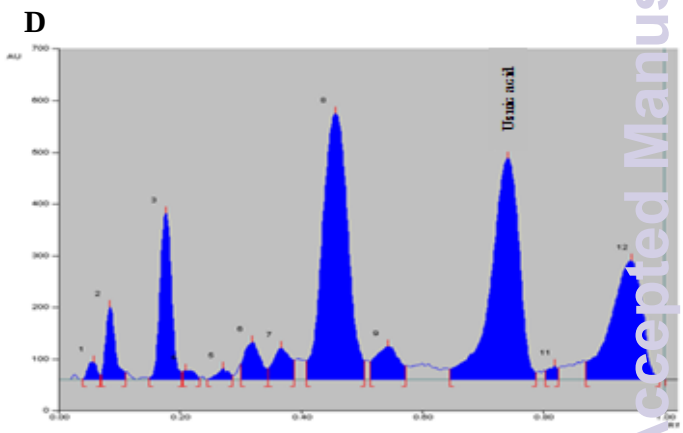

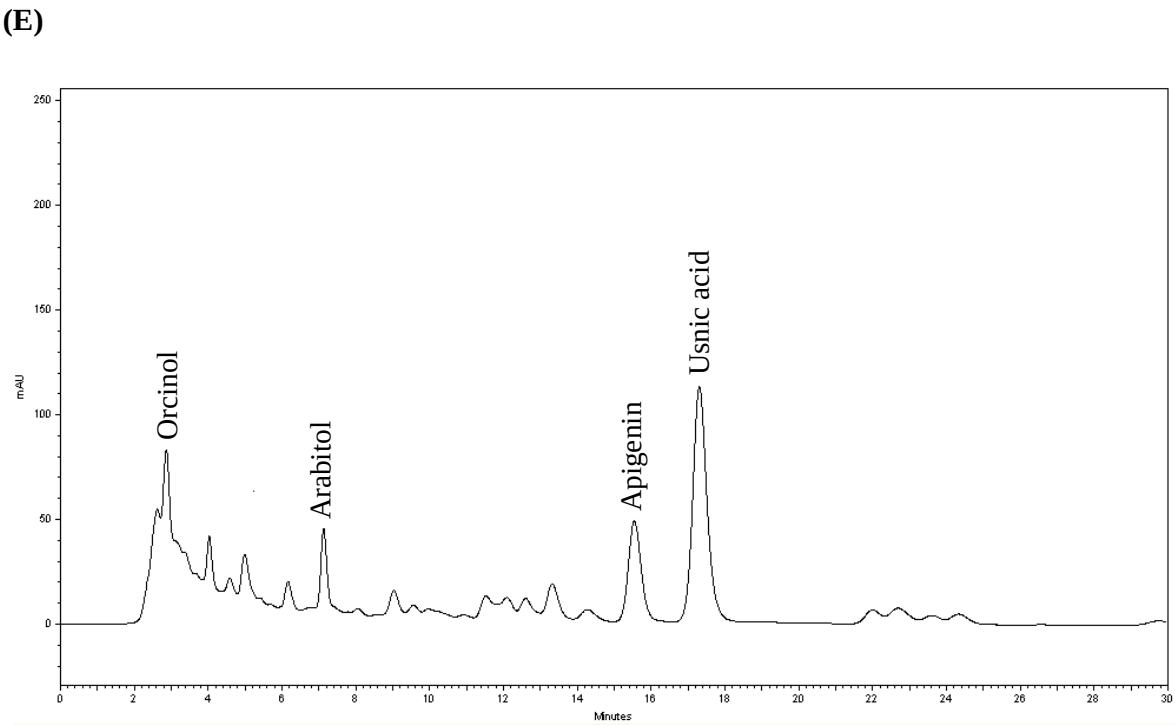

Fig. 4

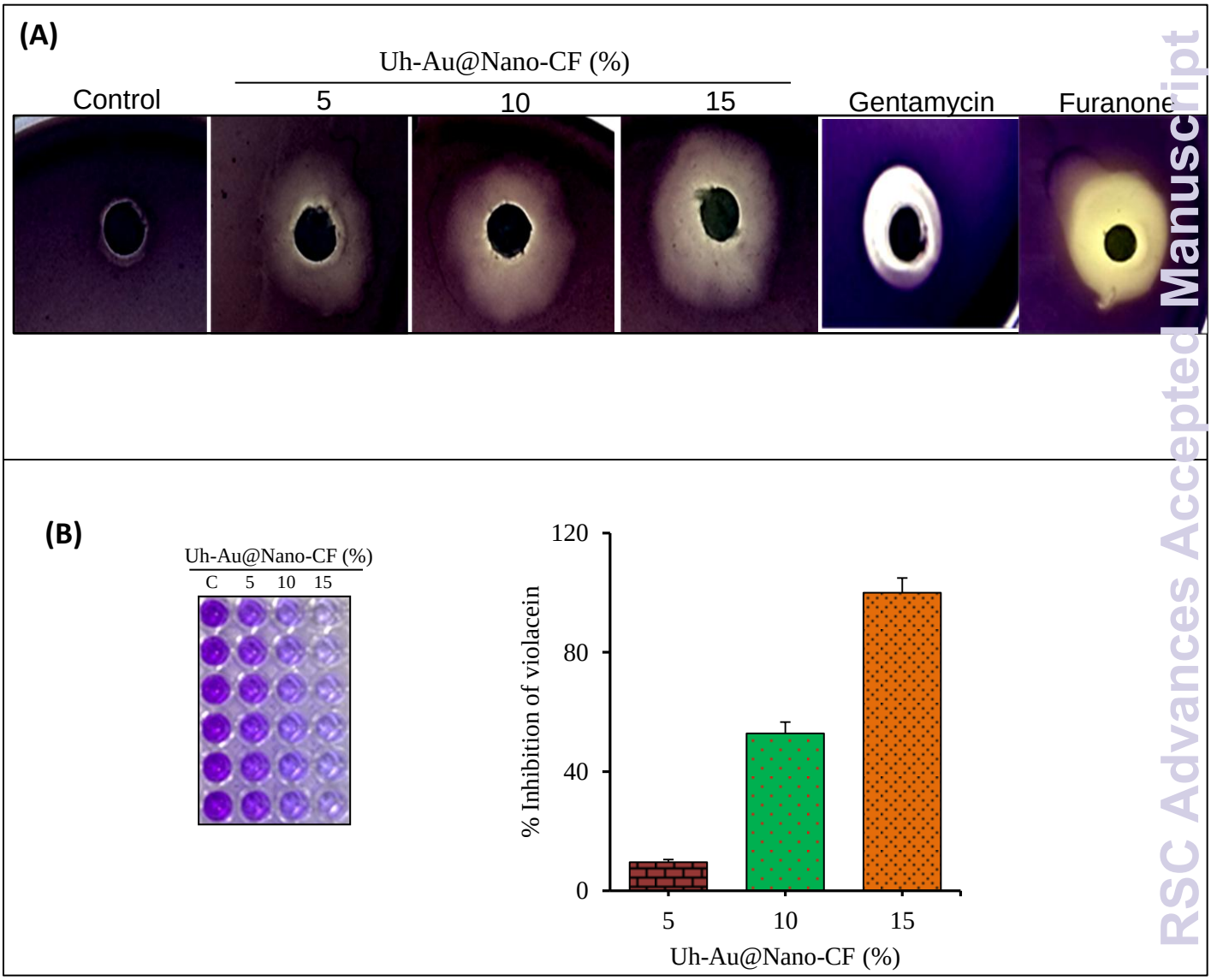

Fig. 5

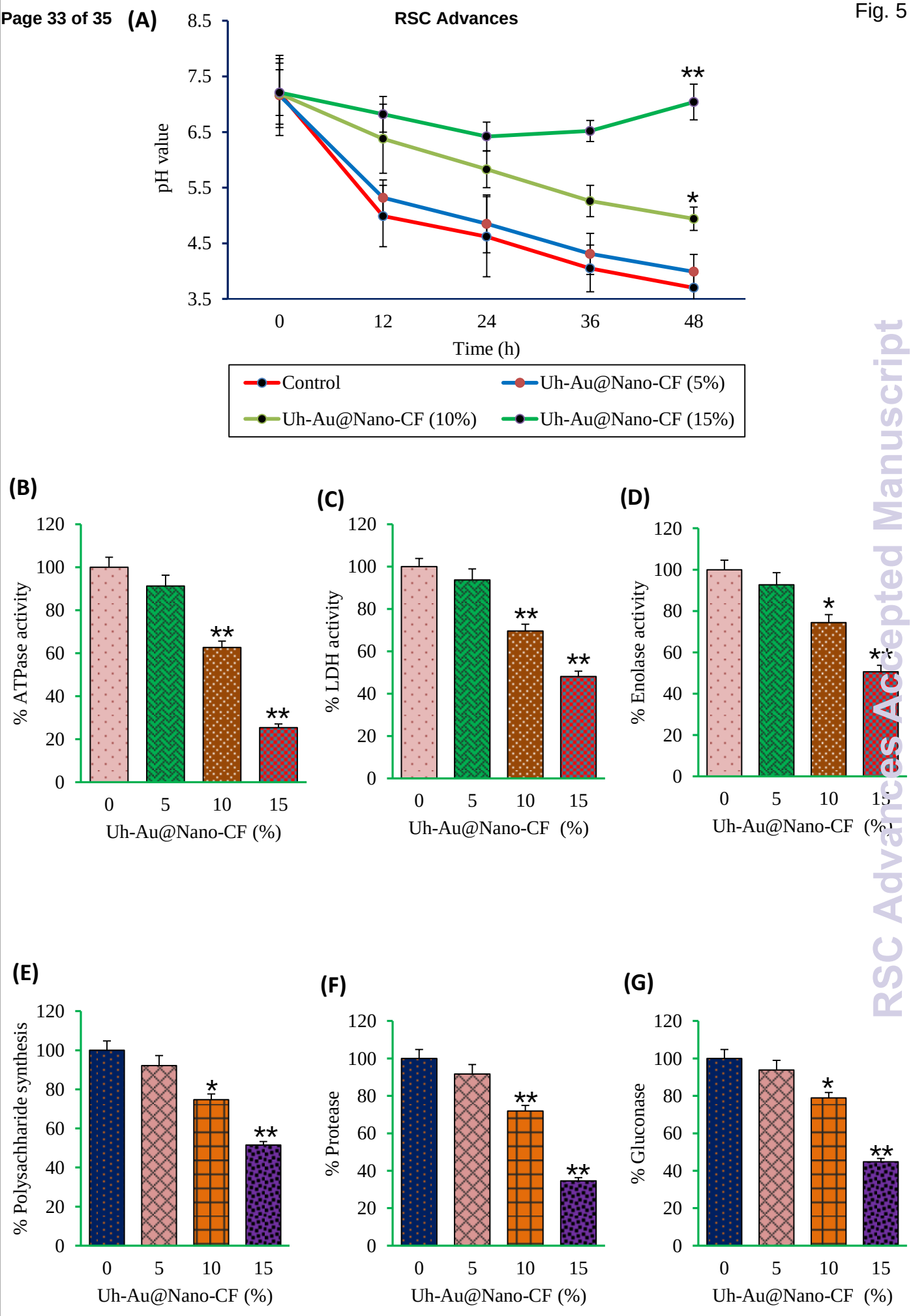

Fig. 6